HHS Public Access

Author manuscript

Clin Exp Optom. Author manuscript; available in PMC 2022 May 01.

Published in final edited form as:

Clin Exp Optom. 2021 May ; 104(4): 523–531. doi:10.1080/08164622.2021.1878827.

Visual function in guinea pigs: behavior and electrophysiology

Ashutosh Jnawali BOptom, PhD, **Sudan Puri BOptom, OD PhD**, **Laura J Frishman, PhD**, **Lisa A Ostrin, OD PhD**

University of Houston College of Optometry, Houston, Texas, USA

Abstract

Clinical relevance: Guinea pig visual function is characterised based on behavioral and electrophysiology measures and retinal ganglion cell density is examined to further develop the guinea pig as a model of human ocular conditions.

Background: Guinea pigs are an important model of human ocular conditions. Here, guinea pig spatial frequency discrimination, pattern and full field photopic electroretinography (ERG), and retinal ganglion cell distribution were investigated.

Methods: Adult guinea pigs (n = 6) were included. Optomotor responses to square wave gratings from 0.3 to 2.4 cycles per degree (cpd) were assessed. Pattern ERG responses were recorded using square wave gratings from 0.025 to 0.25 cpd at 100% contrast, alternating at a temporal frequency of 1.05 Hz. Full field ERG responses were recorded using a 10.0 cd.s/m^2 flash. Ganglion cell density was determined histologically from retinal whole mounts.

Results: Maximum spatial frequency discrimination was 1.65 ± 0.49 cpd for stimuli rotating temporally to nasally and 0.75 ± 0.16 cpd for stimuli rotating nasally to temporally. For pattern ERG, a maximum amplitude of 3.50 ± 1.16 μV for the first negative to positive peak (N1P1) was elicited with a 0.025 cpd grating, and 2.5 ± 0.1 μV for the positive to second negative peak (P1N2) was elicited with a 0.05 cpd grating. For full field ERG, a-wave amplitude was 19.2 ± 4.24 μV, b-wave amplitude was 33.6 ± 8.22 μV, and the PhNR was 24.0 ± 5.72 μV. Peak retinal ganglion cell density was 1621 ± 129 cells/mm^2, located 1–2 mm superior to the optic nerve head.

Conclusion: Guinea pigs show directional selectivity for stimuli moving in the temporal to nasal visual field. Guinea pigs demonstrate a quantifiable PhNR in the full field ERG and negative and positive waveforms in the pattern ERG. The visual streak is located in the superior retina.

Keywords

electroretinogram; guinea pigs; optomotor response; retinal ganglion cells; visual function

Guinea pigs are an important and commonly used animal model of human ocular conditions, such as myopia, and ocular growth related developmental studies of structures such as cornea, crystalline lens and retina.[1–5] Guinea pigs are precocial animals with a well-developed visual system at birth, showing both structural and functional retinal maturity.[6–8]

[Corresponding author] Lisa Ostrin, lisa.ostrin@gmail.com.

Unlike rats and mice that are nocturnal, guinea pigs are crepuscular (i.e. most active at dawn and dusk).

The guinea pig retina is rod dominated; 8–17% of the photoreceptors are cones, depending on the retinal location.[9] They have dichromatic vision with two types of cones, short and medium wavelength sensitive, having peak spectral sensitivities of 429 nm and 529 nm respectively, similar to those of primate retina.[10] Benefits of the guinea pig model include easy breeding, developmental maturation at the age of five months, docile temperament, and wide availability.[11] However, several aspects of guinea pig visual function and ocular structure have not been fully characterised.

In rodents, spatial frequency discrimination can be assessed rapidly using an optomotor paradigm,[12–14] which utilises reflexive movements of the head or body that occur when the environment is moving or drifting across the retina.[15] Using this method, mice and rats have been shown to have a spatial frequency discrimination of approximately 0.4 and 0.6 cycles per degree, respectively.[16,17] The limits of grating acuity using optomotor responses have not yet been reported in guinea pigs, which would be valuable to know in studies related to eye growth and myopia.

Electroretinography provides a non-invasive objective assessment of retinal function, which is useful in investigating the progression of disease. The full field photopic flash electroretinogram (ERG) elicits a retinal response with components representing inner and outer cell types.[18,19] The guinea pig photopic ERG has been shown to be similar to that of humans, in that the ISCEV photopic responses, luminance response function, and oscillatory potentials are comparable.[19]

Guinea pig photopic ERGs in the presence of intravitreal injections of blockers of the ON and OFF retinal pathways were similar to those from human eyes with retinopathies known to have anomalies of those pathways, such as congenital stationary night blindness and cone dystrophy.[19] The a-wave in guinea pigs includes negative-going contributions from second order neurons, hyperpolarising bipolar cells, in addition to photoreceptors, similar to non-human primates.[18] Another component of photopic ERG in the mammalian retina is the photopic negative response (PhNR), which has been shown to be related to retinal ganglion cells in primates and mice.[20–22] However, this component has not yet been reported in guinea pigs.

Characterisation of the PhNR response in guinea pigs would be useful to study the integrity of inner retina in pathological conditions, such as glaucoma. Additionally, no study has yet reported pattern ERG responses in guinea pigs. The pattern ERG is a retinal bio-potential evoked by temporally modulated patterned stimulus,[23] and has been shown to arise primarily from the retinal ganglion cells in mammalian retina.[24–28] In mammals, the pattern ERG has been used as a tool to investigate retinal ganglion cell dysfunction in conditions such as glaucoma.[29]

Structurally, guinea pigs have been shown to possess a visual streak; however, the location and cell density are conflicting between studies.[30,31] Do-Nascimento et al.[30] demonstrated the visual streak to be in the superior retina in guinea pigs, but Choudhury et al.[31] reported

the presence of visual streak in guinea in the inferior retina. Rats and mice do not have a fovea or a well-defined visual streak,[32,33] while rabbits have been shown to possess a visual streak in the retina below the optic nerve head.[34]

The goals of this study were to investigate spatial frequency discrimination using optomotor responses, to characterise the pattern ERG and PhNR responses, and to describe retinal ganglion cell density distribution histologically in adult guinea pigs. These findings will help to further establish the guinea pig as a model of human ocular function and disease.

Methods

Animals

Six healthy adult female pigmented Hartley guinea pigs (Elm Hill Labs, Chelmsford, MA, USA), aged 2.5 years, were included in this study. The mean weight of the animals was 1006 ± 111 gm. Animals were kept under a 12-hour light/dark cycle and provided food and water *ad libitum*. Procedures were approved by the Institutional Animal Care and Use Committee at the University of Houston.

Optomotor responses

Visual performance was assessed behaviorally using a custom optomotor instrument, consisting of a motorised cylindrical drum of 55 cm diameter with a central stationary platform. Square wave gratings for spatial frequencies from 0.3 to 2.4 cycles per degree (cpd) in steps of 0.3 cpd, were printed at 100% contrast on photographic paper and used to line the inside of the drum. The gratings were calibrated for spatial frequencies at the center of the drum. Awake animals were placed on the central stationary platform in a plastic beaker (Figure 1).

The drum was kept in the middle of the room while testing to ensure that the inside of the drum was evenly illuminated. The drum was rotated at a constant speed of 12 degrees per second in both clockwise and counterclockwise directions. The rotation speed was selected based on the literature where a similar setup was used to assess head tracking responses in rats and mice,[12,13] and was confirmed to be an adequate drift speed for guinea pigs in preliminary testing.[35] The tracking response of each animal to the rotating stimulus was evaluated by an experienced investigator observing head rotation. The test was repeated three times for each direction of rotation and for each spatial frequency. Eyes were tested both monocularly and binocularly, and the maximum spatial frequency that elicited observable tracking response in each direction was recorded.

To confirm the maximum spatial frequency that elicited an observable optomotor response, spatial frequency was increased until no head tracking response was observed, and the testing spatial frequency was reduced until a definite response was observed again. For monocular testing, one eye was occluded using a black piece of cloth that was fixed over the eye with surgical tape around the edges.

Electroretinography

For electroretinography (ERG), animals were anesthetised with ketamine (30 mg/kg, Vedco Inc, Saint Joseph, MO, USA) and xylazine (3 mg/kg, Lloyd Laboratories, Philippines) subcutaneously; anesthesia was maintained with a 50% dose every 40 minutes, as needed, via a subcutaneous needle fixed in the back. Pupils were dilated with 1% tropicamide (Bausch and Lomb, Garden City. NY, USA) for both flash and pattern ERGs. ERG responses were obtained under light adapted conditions in room illumination of approximately 300 lux using the Celeris rodent system (Celeris, Diagnosys, LLC, Lowell, MA, USA).

Animals were adapted to room illumination for at least two hours. Pattern ERGs were recorded from each eye, followed by flash ERGs. For pattern ERG, the stimulator probe, designed with a pinhole aperture, was placed in contact with the cornea, aligned with the center of the pupil, and the reference electrode was placed on the fellow eye. Artificial tears (Refresh Liquigel, Allergan) were applied to both eyes to maintain corneal hydration. A ground electrode was inserted under the skin on the fore limb. The built-in heating function of the stage of the instrument was used to maintain the body temperature at 37ºC.

Stimuli consisted of square wave gratings of frequencies ranging from 0.025 to 0.25 cycles per degree at 100% contrast, modulated at a temporal frequency of 1.05 Hz, and 1800 responses were averaged for each eye. Based on schematic eye calculations of the guinea pig eye and an axial length of 8.64 mm, the gratings stimulated an area of approximately 4 × 4.6 mm in the central retina.[36–38] For the pattern ERG, the system used a filter with low frequency cutoff of 0.125 Hz and high frequency cutoff of 100 Hz. The intersweep delay was 0 s and first sweep delay was 6000 ms. The frame rate was 66.62 Hz and viewing angle was 21˚ horizontal × 16˚ vertical.

For the flash ERG, stimulator probes were placed in contact with each cornea, aligned with the center of the pupil, and responses were collected from both eyes simultaneously. Flash luminance energy of 10.0 cd.s/m^2 with background intensity of 9.0 cd/m^2 was used; this luminance energy was previously shown to elicit ERG b-waves of near maximal amplitude in the guinea pig.[19] The interstimulus interval was 1 s, and 10 responses were averaged for each eye. To assess repeatability, ERG responses were recorded from the same six animals on two occasions, separated by at least a week.

ERG responses were analysed using a custom written program in MATLAB (The MathWorks, Inc., Natick, MA, USA). For flash ERGs, a-wave amplitudes were measured from baseline to the a-wave trough on the raw trace (drift correction and 60 Hz notch filter only). For b-wave and PhNR measurement, a band pass filter of 1–50 Hz was applied to the raw trace. A 50 Hz cutoff was used for the b-wave and PhNR to minimize effects of oscillatory activity on amplitude measurements. The b-wave amplitude was measured from a-wave trough to the b-wave peak. The PhNR was measured from baseline to the trough immediately following the b-wave.

For pattern ERG recordings, drift correction, 60 Hz notch filter, and a band pass filter of 1–100 Hz were applied to the raw traces. The first negative trough (N1), the first positive peak

(P1), and the second negative trough (N2) were identified; the amplitudes and implicit times were measured for each waveform, as well as for the N1P1 and P1N2 excursions.

Ganglion cell quantification

Animals (n = 4 of the 6 guinea pigs) were euthanised with intraperitoneal injections of 100 mg/kg sodium pentobarbital (Fatal-Plus or Euthasol, Vortech Pharmaceuticals, Dearborn, MI, USA), and one eye each was randomly chosen and marked for orientation, enucleated, and placed in phosphate buffered saline (PBS) solution. Eyes were fixed in 4% paraformaldehyde for two hours, orientation cuts were made, and the tissue was washed with PBS and PBS with tritonX.

The whole eyecups with orientation cuts were then immersed in blocking buffer solution for at least an hour, and transferred to rounded bottomed tubes containing primary antibody, alpha-RBPMS (retinol binding protein with multiple splicing) rabbit antibody (Ab) (Abcam, Cambridge, MA, USA), a specific marker for retinal ganglion cells, at 1:500 dilution. The eyecups were kept on rotator at 4°C for five days. On the sixth day, eyes were washed with PBS and PBS with tritonX, and vitreous was removed under a light microscope (DM1000, Leica, Wetzlar, Germany). Eyecups were labeled with secondary antibody, goat anti-rabbit alexa fluor 488 (ThermoFisher Scientific, Grand Island, NY, USA) at 1:250 dilution for two hours followed by a PBS with tritonX wash.

Under low illumination, retina was isolated from the retinal pigment epithelium and choroid and mounted on glass slides using cytoseal mounting medium (Richard-Allan Cytoseal 60, ThermoFisher Scientific, Grand Island, NY, USA). The slides were incubated in the dark overnight and imaged on DeltaVision wide field deconvolution fluorescence microscope (GE Life Sciences, Pittsburg, PA, USA) at 20x magnification the following day.

Images were collected as panels for the retinal flat mounts under 20X. The panels were stitched together for the composite image, and saved as JPEG images (Figure 2A). The images were then imported in Fiji (ImageJ, NIH, Bethesda, MD, USA).[39] Grids with boxes of size 250 × 250 μm^2 were overlaid over the entire retinal flat mount image. Retinal ganglion cells were counted on every third box manually with cell counter in Fiji (Figure 2B). Counts were converted to ganglion cell density in cells/mm^2.

Statistical Analysis

Statistical analysis was performed using MedCalc statistical software version 18 (MedCalc Software, Ostend, Belgium). Data are expressed as mean ± standard deviation. Normality of data was assessed with Shapiro-Wilk test. Spatial frequency discrimination for drift direction was assessed with paired t-tests. The intersession repeatability of ERG amplitudes was assessed with coefficient of variation based on mean of two recording sessions for all eyes. Repeated measures ANOVA was used to assess the amplitude of pattern ERG components N1P1 and P1N2 with spatial frequency.

Results

Optomotor responses

Results for behavioral assessment of vision using an optomotor paradigm are shown in Figure 3. With binocular viewing, the mean maximum spatial frequency to elicit a tracking response was 1.65 ± 0.49 cpd, which was the same as that obtained with monocular viewing when the stimulus rotated in the temporal to nasal direction. Similar binocular and monocular tracking is likely due to the limited overlap in the visual fields of the two eyes. However, when the stimulus rotated in the nasal to temporal direction under monocular viewing, the mean maximum spatial frequency to elicit tracking decreased to 0.75 ± 0.16 cpd, which was significantly lower than the temporal to nasal direction ($p < 0.001$), demonstrating a directional selectivity for stimuli rotating towards the midline.

Electroretinography

Representative flash and pattern ERG traces are shown in Figure 4. Results from right eyes are reported. Response amplitudes and implicit times for the a-wave, b-wave, and PhNR of the flash ERG are summarised in Table 1. Mean a-wave amplitude was 19.2 ± 4.2 μV, b-wave amplitude was 33.6 ± 8.2 μV, and the PhNR was 24.0 ± 5.7 μV. Mean implicit times for the a-wave, b-wave, and PhNR were 13.7 ± 0.9 ms, 32.3 ± 2.3 ms, and 54.1 ± 2.2 ms, respectively. For repeat measures, the coefficient of variation with 95% confidence intervals for a-wave, b-wave, and PhNR amplitudes were 15.4% (3.5–27.3%), 19.3% (4.3–34.2%), and 22.6% (5.1–40.1%), respectively.

Response amplitudes and implicit times for N1, P1, N2, N1P1, and P1N2 of the pattern ERG are summarised in Table 2. Repeated measures ANOVA showed that the amplitude for both N1P1 and P1N2 are dependent on spatial frequency ($p < 0.001$ and $p = 0.001$, respectively). N1P1 reached a maximum amplitude of 3.5 ± 1.2 μV at the lowest spatial frequency tested (0.025 cpd, Figure 5A). The amplitude reduced by almost half for the next spatial frequency of 0.05 cpd (1.7 ± 1.0 μV), and remained relatively stable at further higher spatial frequencies of 0.075, 0.1, and 0.125 cpd. The N1P1 amplitude for a 0.25 cpd stimulus further reduced to 0.5 ± 0.2 μV.

For N2, the results were more variable, and a consistent negative trough below the baseline was not always present. Thus, the positive values for N2 amplitude represent the trough immediately following the P1 peak that did not cross the baseline. For this reason, P1N2 was used to describe the N2 responses following the P1 peak. The peak amplitude of P1N2 was obtained at 0.05 cpd spatial frequency, and responses for spatial frequencies either larger or smaller than 0.05 cpd were attenuated (Figure 5B). The mean implicit time for P1 and N2 for the optimal stimulus of 0.05 cpd at 100% contrast were 50.3 ± 1.9 ms and 88.0 ± 3.2 ms, respectively. The co-efficient of variation with 95% confidence intervals for N1P1 and P1N2 amplitudes were 24.4% (0–36.5%) and 39.2% (0–58.6%) respectively.

Ganglion cell quantification

A representative retinal ganglion cell density heat map from left eye of one guinea pig is shown in Figure 6. The mean peak retinal ganglion cell density for all eyes was 1621 ± 129

cells/mm^2, and was located in a similar location across all eyes, approximately 1–2 mm superior to the optic nerve head and extended laterally on either side, approximately 8–10 mm, towards the nasal and temporal retina, representing the visual streak.

Discussion

The main goals of this study were to describe visual function in guinea pigs using behavioral and electrophysiological measures. The spatial frequency sensitivity in adult guinea pigs was determined with optomotor responses. Partial directional selectivity was observed. The presence of a quantifiable and relatively repeatable photopic negative response (PhNR) and pattern ERG responses was demonstrated. The location of visual streak was identified to be in the superior retina using a specific marker for retinal ganglion cells. Findings from this study will be important for future studies evaluating retinal functional changes in guinea pigs in conditions such as myopia, optic neuropathy, and glaucoma.

A custom optokinetic instrument was utilised to assess behavioral visual function in guinea pigs, and fa maximum spatial frequency discrimination of approximately 1.6 cycles per degree was found, determined by evaluating head tracking responses to drifting gratings in both clockwise and counterclockwise directions.

Assessment of acuity in rodents using optomotor responses is a well-established technique; it has also been used in rabbits,[40] zebrafish,[41] and chicks.[42] Cowey, et al. first demonstrated such tracking responses in rats to drifting gratings and found that tracking was lost in eyes with complete sectioning of optic nerve.[13] Similarly, Thaung, et al. demonstrated that optomotor responses could be used to differentiate between mice with normal vision and those with severe retinal degeneration.[12] The maximum spatial frequency discrimination with gratings in wild type mice has been reported to be 0.5 cpd.[43] Prusky, et al, used a virtual optomotor system to demonstrate a maximum grating acuity of 0.4 cpd.[16]

Interestingly, under monocular conditions, an optokinetic response in mice and rats is elicited only when the stimulus is rotating in the temporal to nasal visual field.[13,17] The lack of a response to stimuli rotating in the nasal to temporal direction is attributed to having only crossed subcortical projections from the eyes,[17,44] and may be an evolutionary adaptation for lower mammals of prey. In higher mammals, such as felines and primates, monocular optokinetic responses have been shown to be similar to either direction of motion.[45,46]

Directional selectivity in guinea pigs was also observed. However, unlike in rats and mice, the directional selectivity in guinea pigs was not complete. Rather, the mean spatial frequency sensitivity measured with gratings drifting from nasal to temporal visual field for each eye was approximately half of the sensitivity for temporal to nasal rotation. This suggests that there may be a sufficient ipsilateral projection from each eye to the visual cortex to allow spatial frequency discrimination in either direction.[47] Although the directional selectivity in guinea pigs in this study was not found to be as complete as in other rodents, the partial directional selectivity allows the visual capabilities of each eye to be measured under binocular conditions by changing the direction of rotation.

The light adapted flash ERG showed that a- and b-wave amplitudes in the pigmented guinea pigs in the present study were approximately 19 μV and 34 μV, respectively. Previous studies have reported amplitudes for a- and b-waves in response to flashes of similar luminance energy, and slightly higher background luminance in albino guinea pigs to be approximately 40 μV and 111 μV, respectively.[18,19]

Racine, et al. compared the ERG responses between humans, guinea pigs, rats, and mice using similar stimulus conditions for all species, and concluded that guinea pigs represent a superior rodent model of human photopic ERG.[19] Vingrys et al. also reported larger ERG waveforms in albino guinea pigs compared to those found here.[48] Previous investigators noted that ERG waveforms were larger, faster and more sensitive in albino guinea pigs than pigmented animals.[48,49] Similar observations of larger flash ERG waveforms have been reported in albino human subjects compared to pigmented control subjects.[50,51]

Some of the reasons speculated for such differences include more light entering the eye in albinos through translucent iris, greater fundal reflectance and light scatter due to poor retinal pigment absorption, and reduced ocular resistance due to less concentration of melanin and greater light effectiveness.[49–51] These differences across pigmented and albino strains, as well as differences in instruments and electrodes, may account for reported differences in amplitudes between studies. Amplitudes observed here are also much smaller than those found for mice and humans,[19,28] and more similar to those reported in rabbits[52] that, like guinea pigs, possess an avascular retina. In addition to instrument related differences, difference in the amplitudes between species could be due to varying contribution of the different retinal neurons for the a- and b-wave components of the flash ERG.

The PhNR of the full field ERG is the immediate negative trough following the b-wave.[21] In non-human primates and humans, the PhNR is known to originate from retinal ganglion cells.[20,21] Previous studies evaluating the ERG in guinea pigs have not reported a PhNR.[18,19,49,53] The present authors observed a consistent PhNR after the b-wave in guinea pigs, similar to that reported in non-human primates and humans.[20,21] The implicit time for the PhNR in guinea pigs in this study was 54 ms, slightly earlier that reported in non-human primates and humans.[20,21] This is relatively shorter compared to longer time in mice of 150 ms.[22]

The mean PhNR amplitude of 24 μV in guinea pig in this study is greater than the value of 16 μV reported by Viswanathan, et al. for normal macaque retina with brief flash of 1.9 log phot td sec,[21] but similar to that reported in humans, in the range of 15–30 μV.[20] With similar flash luminance energy of 10 cd.s/m^2 as used in this study, Liu et al. reported mean PhNR amplitude of approximately 19 ± 11 μV in mice.[54] The presence of the PhNR in guinea pigs might provide a metric to assess inner retinal function, as has been reported in non-human primates, humans and mice, and therefore, future studies aimed at determining the origin of the PhNR in guinea pigs would be valuable.

Pattern ERG responses in guinea pigs have not been reported previously. Pattern ERG waveforms were found to be similar in shape to those from other mammalian species

including mice, rats, non-human primates, and humans, with an initial negative trough (N1), positive peak (P1), and second negative trough (N2).[23,27,55,56] In humans, these waveforms are referred to as N35, P50, and N95, respectively, with the numbers referring to the average time of peak for those components.[23] Here, a 0.025–0.05 cpd grating was the optimal stimulus size to elicit a maximum pattern ERG response.

The amplitudes of P1 and P1N2 in guinea pigs were similar to those found in humans and non-human primates,[23,56] as well as rabbits.[57] However, amplitudes have been shown to be higher in mice and rats.[28,58] The peak P1 and P1N2 amplitude in mice with square wave gratings of 0.05 cpd at 90% contrast and 1 Hz reversal rate with mean luminance of 50 cd/m^2 were reported to be 7.4 μV and 13.3 μV, respectively.[28] In rats, peak P1N2 amplitude was reported to be 10 μV with a checkerboard pattern of 99% contrast alternating at 6.1 Hz at mean luminance of 100 cd/m^2.[58] In rabbits, another species with avascular retina, mean amplitudes for P1 and N2 were reported to be 1.8 μV and 2.3 μV respectively, using square wave gratings of 0.15 cpd and of 1.5 Hz reversal at mean luminance of 221 cd/m^2 and contrast of 71%.[57]

In non-human primates, using a checkerboard pattern of 1˚ at 84% contrast and 2 Hz reversal rate and mean luminance of 55 cd/m^{2,} the mean P50 amplitude was reported to be 3.6 μV.[56] In humans, ISCEV (International Society for Clinical Electrophysiology of Vision) reports the average amplitude for P50 between 2 to 8 μV.[23] Thus, compared to rats and mice, guinea pig pattern ERG amplitudes are comparable to those of rabbits, non-human primates, and humans. Likewise, the mean implicit time for these components in guinea pigs were similar to humans, but were different from those in mice and rats.[28,56] Mean P1 implicit time in mice for maximum contrast stimulus was reported to be around 60 ms and that for N2 around 132 ms.[28] In non-human primate, implicit time for P1 and N2 are reported to be around 50 and 114 ms, respectively,[56] while those for humans are 50 and 95 ms. In this study, the mean implicit times for P1 and N2 in guinea pig pattern ERG for a stimulus of 0.1 cpd at 100% contrast were around 50 and 90 ms, respectively, which are similar to those from human responses.

Thus, guinea pig pattern ERG responses are more comparable in amplitude and implicit times to humans and non-human primates than to mice and rats. In mice and monkeys, the retinal source of origin of pattern ERG has been determined to be retinal ganglion cells.[28,59] The demonstration of the presence of pattern ERG in guinea pigs in this study opens possibilities for further studies investigating the retinal origin of these waveforms, not yet established in guinea pig, and their implications in retinal disease.

A mean peak retinal ganglion cell density of approximately 1621 cells/mm^2 was found in this work, with the maximum of 1760 cells/mm^2 in one animal, which approaches the peak density reported by Rodriguez, et al (2064 cells/mm^2), using a similar staining technique.[60] Retinol binding protein with multiple splicing (RBPMS) antibody has been shown to be a highly specific marker for retinal ganglion cells in the mammalian retina including rats, mice, rabbit, macaque, and guinea pigs.[60] Do-Nascimento et al. reported peak retinal ganglion cell density of 2272 cells/mm^2.[30] However, they used Nissl stain for quantification of ganglion cells, which is a non-specific marker for nucleic acid and stains all nuclei.

Since the retinal ganglion cell layer contains a large proportion of displaced amacrine cells, [30] it is likely the retinal ganglion cell count obtained with Nissl staining was confounded by the amacrine cell population. Because of the use of markers not specific to retinal ganglion cells, authors relied on morphological clues such as cell body diameter, color of nucleus, and prominence of nucleolus to differentiate between ganglion cells and other neurons.

On the other hand, Choudhury, et al. reported a peak retinal ganglion cell density of 720–864 cells/mm^2.[31] This lower density could be due to not taking into account retinal ganglion cell with small cell bodies.[30] The location of the visual streak in the guinea pig retina was reported to be in different locations by two earlier studies. Do-Nascimento, et al.[30] reported the visual streak to be in the superior retina in guinea pigs, and our results confirm this finding. In contrast, Choudhury, et al.[31] reported the presence of visual streak in guinea in the inferior retina.

A peak retinal ganglion cell density of 1760 cells/mm^2 predicts a maximum spatial frequency discrimination of 2.07 cpd, with a calculated retinal magnification factor of 99 microns per degree, or 4.15 cells per degree (1760 cells/mm^2 = 42 cells/mm, retinal magnification factor = 0.099 mm/deg, sampling density = cells/mm × mm/deg = 42 × 0.099 = 4.15 cells/deg).[30] With optomotor responses, a mean spatial frequency discrimination of 1.64 cpd was found, and with pattern ERG, a response was elicited with a maximum spatial frequency grating of 0.05 cpd. The estimated spatial frequency discrimination from retinal ganglion cell density represents the upper limits of vision, and behavioral measurements can yield lower values due to the limitations imposed by optical imperfections and neural factors.[61]

The spatial frequency discrimination determined with optomotor tracking depends, especially in lower vertebrates, on properties of the retinal efferent pathways to subcortical structures.[61] The nucleus of the optic tract and the dorsal terminal nucleus of the accessory optical system are involved in the optomotor tracking responses.[17,62] The cells in the nucleus of the optic tract and the dorsal terminal nucleus have large receptive fields, thus yielding lower spatial frequency preference. [17] Similarly, detection of pattern ERG responses is dependent on several factors, including instrument specific variables and electrode sensitivity, and retinal cells of origin of the response, not yet established, and therefore, may result in lower spatial frequency discrimination than that predicted solely by retinal ganglion cell density.

The current study has the following limitations. Only female guinea pigs were used in this study. However, functional differences between males and females are not expected, and a few earlier studies using both male and females have not suggested any differences in electrophysiological responses between the two.[29,63]

For optokinetic measures, the motor of the rotating drum could be heard. It is unlikely that the animals tracked the grating when the motor was on because significant and consistent spatial frequency cut offs were observed based on direction and grating size. Head tracking was confirmed by visual observation. While automated video tracking would have been

more objective, the observer was experienced and could reliably detect tracking vs not tracking.

For ERGs, only light adapted responses were tested, which allowed the PhNR to be probed and pattern ERG responses to be examined. Guinea pig scotopic ERGs have been reported previously,[64] but further studies including mesopic testing would provide future insight in guinea pig visual function. Finally, our sample size was small, and this may have contributed to the variability in results.

Conclusion

This study characterised guinea pig visual function using behavioral and electrophysiological methods, and confirmed the location of visual streak in the superior retina in the guinea pig retina with markers selective for retinal ganglion cells. The findings suggest that spatial frequency discrimination can be rapidly assessed in guinea pigs using optomotor responses. The presence of a PhNR in the full field flash ERG and pattern ERG responses in guinea pigs, and the similarity of these waveforms to those in primates, further supports the use of guinea pigs as a model of human ocular disease.

ACKNOWLEDGEMENTS

This study was funded by NIH NEI K08 EY022696 and NIH NEI P30 EY007551. The authors thank Alan Burns for help with Delta Vision imaging, Krista Beach for help with immunohistochemistry, John Bauer for help with constructing the custom optokinetic drum, and Alexander Schill for help calibrating the pattern ERG stimulus.

REFERENCES

1. Howlett MH, McFadden SA. Spectacle lens compensation in the pigmented guinea pig. Vision Res 2009; 49: 219–227. [PubMed: 18992765]
2. Howlett MH, McFadden SA. Form-deprivation myopia in the guinea pig (Cavia porcellus). Vision Res 2006; 46: 267–283. [PubMed: 16139323]
3. Garcia MB, Jha AK, Healy KE, et al. A bioengineering approach to myopia control tested in a guinea pig model. Invest Ophthalmol Vis Sci 2017; 58: 1875–1886. [PubMed: 28358959]
4. Jiang L, Long K, Schaeffel F, et al. Disruption of emmetropization and high susceptibility to deprivation myopia in albino guinea pigs. Invest Ophthalmol Vis Sci 2011; 52: 6124–6132. [PubMed: 21666231]
5. McFadden SA, Howlett MH, Mertz JR. Retinoic acid signals the direction of ocular elongation in the guinea pig eye. Vision Res 2004; 44: 643–653. [PubMed: 14751549]
6. Loeliger M, Rees S. Immunocytochemical development of the guinea pig retina. Exp Eye Res 2005; 80: 9–21. [PubMed: 15652521]
7. Spira AW. In utero development and maturation of the retina of a non-primate mammal: a light and electron microscopic study of the guinea pig. Anat Embryol (Berl) 1975; 146: 279–300. [PubMed: 1147288]
8. Huang J, Wyse JP, Spira AW. Ontogenesis of the electroretinogram in a precocial mammal, the guinea pig (Cavia porcellus). Comp Biochem Physiol A Comp Physiol 1990; 95: 149–155. [PubMed: 1968807]
9. Peichl L, Gonzalez-Soriano J. Morphological types of horizontal cell in rodent retinae: a comparison of rat, mouse, gerbil, and guinea pig. Vis Neurosci 1994; 11.
10. Jacobs GH, Deegan JF 2nd. Spectral sensitivity, photopigments, and color vision in the guinea pig (Cavia porcellus). Behav Neurosci 1994; 108: 993–1004. [PubMed: 7826522]

11. Zhou X, Qu J, Xie R, et al. Normal development of refractive state and ocular dimensions in guinea pigs. Vision Res 2006; 46: 2815–2823. [PubMed: 16723148]
12. Thaung C, Arnold K, Jackson IJ, et al. Presence of visual head tracking differentiates normal sighted from retinal degenerate mice. Neurosci Lett 2002; 325: 21–24. [PubMed: 12023058]
13. Cowey A, Franzini C. The retinal origin of uncrossed optic nerve fibres in rats and their role in visual discrimination. Exp Brain Res 1979; 35: 443–455. [PubMed: 456452]
14. Abdeljalil J, Hamid M, Abdel-Mouttalib O, et al. The optomotor response: a robust first-line visual screening method for mice. Vision Res 2005; 45: 1439–1446. [PubMed: 15743613]
15. Tauber ES, Atkin A. Optomotor responses to monocular stimulation: relation to visual system organization. Science 1968; 160: 1365–1367. [PubMed: 5651899]
16. Prusky GT, Alam NM, Beekman S, et al. Rapid quantification of adult and developing mouse spatial vision using a virtual optomotor system. Invest Ophthalmol Vis Sci 2004; 45: 4611–4616. [PubMed: 15557474]
17. Douglas RM, Alam NM, Silver BD, et al. Independent visual threshold measurements in the two eyes of freely moving rats and mice using a virtual-reality optokinetic system. Vis Neurosci 2005; 22: 677–684. [PubMed: 16332278]
18. Lei B The ERG of guinea pig (Cavis porcellus): comparison with I-type monkey and E-type rat. Doc Ophthalmol 2003; 106: 243–249. [PubMed: 12737501]
19. Racine J, Joly S, Rufiange M, et al. The photopic ERG of the albino guinea pig (Cavia porcellus): a model of the human photopic ERG. Doc Ophthalmol 2005; 110: 67–77. [PubMed: 16249958]
20. Viswanathan S, Frishman LJ, Robson JG, et al. The photopic negative response of the flash electroretinogram in primary open angle glaucoma. Invest Ophthalmol Vis Sci 2001; 42: 514–522. [PubMed: 11157891]
21. Viswanathan S, Frishman LJ, Robson JG, et al. The photopic negative response of the macaque electroretinogram: reduction by experimental glaucoma. Invest Ophthalmol Vis Sci 1999; 40: 1124–1136. [PubMed: 10235545]
22. Chrysostomou V, Crowston JG. The photopic negative response of the mouse electroretinogram: reduction by acute elevation of intraocular pressure. Invest Ophthalmol Vis Sci 2013; 54: 4691–4697. [PubMed: 23766473]
23. Bach M, Brigell MG, Hawlina M, et al. ISCEV standard for clinical pattern electroretinography (PERG): 2012 update. Doc Ophthalmol 2012; 126: 1–7. [PubMed: 23073702]
24. Mafei L, Fiorentini A. Electroretinographic responses to alternating gratings before and after section of the optic nerve. Science 1981; 211: 953–955. [PubMed: 7466369]
25. Viswanathan S, Frishman LJ, Robson JG. The uniform field and pattern ERG in macaques with experimental glaucoma: removal of spiking activity. Invest Ophthalmol Vis Sci 2000; 41: 2797–2810. [PubMed: 10937600]
26. Dawson WW, Maida TM, Rubin ML. Human pattern-evoked retinal responses are altered by optic atrophy. Invest Ophthalmol Vis Sci 1982; 22: 796–803. [PubMed: 7076425]
27. Berardi N, Domenici L, Gravina A, et al. Pattern ERG in rats following section of the optic nerve. Exp Brain Res 1990; 79: 539–546. [PubMed: 2340873]
28. Miura G, Wang MH, Ivers KM, et al. Retinal pathway origins of the pattern ERG of the mouse. Exp Eye Res 2009; 89: 49–62. [PubMed: 19250935]
29. Cvenkel B, Sustar M, Perovsek D. Ganglion cell loss in early glaucoma, as assessed by photopic negative response, pattern electroretinogram, and spectral-domain optical coherence tomography. Doc Ophthalmol 2017; 135: 17–28. [PubMed: 28567618]
30. Do-Nascimento JL, Do-Nascimento RS, Damasceno BA, et al. The neurons of the retinal ganglion cell layer of the guinea pig: quantitative analysis of their distribution and size. Braz J Med Biol Res 1991; 24: 199–214. [PubMed: 1726652]
31. Choudhury BP. Retinotopic organization of the guinea pig's visual cortex. Brain Res 1978; 144: 19–29. [PubMed: 638761]
32. Salinas-Navarro M, Jimenez-Lopez M, Valiente-Soriano FJ, et al. Retinal ganglion cell population in adult albino and pigmented mice: a computerized analysis of the entire population and its spatial distribution. Vision Res 2009; 49: 637–647. [PubMed: 19948111]

33. Jeffery G The relationship between cell density and the nasotemporal division in the rat retina. Brain Res 1985; 347: 354–357. [PubMed: 4063814]
34. Davis FA. The anatomy and histology of the eye and orbit of the rabbit. Trans Am Ophthalmol Soc 1929; 27.
35. Ostrin LA, Mok-Yee J, Wildsoet CF. Behavioral measures of spatial vision during early development in pigmented and albino guinea pigs. Invest Ophthalmol and Vis Sci 2011; 52.
36. Jnawali A, Beach KM, Ostrin LA. In vivo imaging of the retina, choroid, and optic nerve head in guinea pigs. Curr Eye Res 2018; 43: 1006–1018. [PubMed: 29641938]
37. Howlett MH, McFadden SA. Emmetropization and schematic eye models in developing pigmented guinea pigs. Vision Res 2007; 47: 1178–1190. [PubMed: 17360016]
38. Bennett AG. A method of determining the equivalent powers of the eye and its crystalline lens without resort to phakometry. Ophthalmic Physiol Opt 1988; 8: 53–59. [PubMed: 3047630]
39. Schindelin J, Arganda-Carreras I, Frise E, Kaynig V, et al. Fiji: an open-source platform for biological-image analysis. Nat Methods 2012; 9: 676–682. [PubMed: 22743772]
40. Fuller JH. Head movements during optokinetic stimulation in the alert rabbit. Exp Brain Res 1987; 65: 593–604. [PubMed: 3556487]
41. Maurer CM, Huang YY, Neuhauss SC. Application of zebrafish oculomotor behavior to model human disorders. Rev Neurosci 2011; 22: 5–16. [PubMed: 21615257]
42. Schmid KL, Wildsoet CF. Assessment of visual acuity and contrast sensitivity in the chick using an optokinetic nystagmus paradigm. Vision Res 1998; 38: 2629–2634. [PubMed: 12116708]
43. Schmucker C, Seeliger M, Humphries P, et al. Grating acuity at different luminances in wild-type mice and in mice lacking rod or cone function. Invest Ophthalmol Vis Sci 2005; 46: 398–407. [PubMed: 15623801]
44. Thomas BB, Seiler MJ, Sadda SR, et al. Optokinetic test to evaluate visual acuity of each eye independently. J Neurosci Methods 2004; 138: 7–13. [PubMed: 15325106]
45. Tusa RJ, Demer JL, Herdman SJ. Cortical areas involved in OKN and VOR in cats: cortical lesions. J Neurosci 1989; 9: 1163–1178. [PubMed: 2703872]
46. Zee DS, Tusa RJ, Herdman SJ, et al. Effects of occipital lobectomy upon eye movements in primate. J Neurophysiol 1987; 58: 883–907. [PubMed: 3681400]
47. Jen LS, So KF, Chang AB. An anterograde HRP study of the retinotectal pathways in albino and pigmented guinea pigs. Brain Res 1983; 263: 331–335. [PubMed: 6301649]
48. Vingrys AJ, Bui BV. Development of postreceptoral function in pigmented and albino guinea pigs. Vis Neurosci 2020;18: 605–13.
49. Bui BV, Vingrys AJ. Development of receptoral responses in pigmented and albino guinea-pigs (Cavia porcellus). Doc Ophthalmol 1999; 99: 151–170. [PubMed: 11097119]
50. Russell-Eggitt I, Kriss A, Taylor DS. Albinism in childhood: a flash VEP and ERG study. Br J Ophthalmol 1990; 74: 136–40 [PubMed: 2322509]
51. Krill AE, Lee GB. The electroretinogram in albinos and carriers of the ocular albino trait. Arch Ophthalmol 1963; 69: 32–38. [PubMed: 14035804]
52. Naderian A, Bussieres L, Thomas S, et al. Cellular origin of intrinsic optical signals in the rabbit retina. Vision Res 2017; 137: 40–49. [PubMed: 28687326]
53. Rosolen SG, Rigaudiere F, LeGargasson JF, et al. Comparing the photopic ERG i-wave in different species. Vet Ophthalmol 2004; 7: 189–192. [PubMed: 15091327]
54. Liu Y, McDowell CM, Zhang Z, et al. Monitoring retinal morphologic and functional changes in mice following optic nerve crush. Invest Ophthalmol Vis Sci 2014; 55: 3766–3774. [PubMed: 24854856]
55. Porciatti V The mouse pattern electroretinogram. Doc Ophthalmol 2007; 115: 145–153. [PubMed: 17522779]
56. Luo X, Frishman LJ. Retinal pathway origins of the pattern electroretinogram (PERG). Invest Ophthalmol Vis Sci 2011; 52: 8571–8584. [PubMed: 21948546]
57. Feghali JG, Jin JC, Odom JV. Effect of short-term intraocular pressure elevation on the rabbit electroretinogram. Invest Ophthalmol Vis Sci 1991; 32: 2184–2189. [PubMed: 2071332]

58. Ben-Shlomo G, Bakalash S, Lambrou GN, et al. Pattern electroretinography in a rat model of ocular hypertension: functional evidence for early detection of inner retinal damage. Exp Eye Res 2005; 81: 340–349. [PubMed: 16129101]

59. Maffei L, Fiorentini A, Bisti S, et al. Pattern ERG in the monkey after section of the optic nerve. Exp Brain Res 1985; 59: 423–425. [PubMed: 4029317]

60. Rodriguez AR, de Sevilla Muller LP, Brecha NC. The RNA binding protein RBPMS is a selective marker of ganglion cells in the mammalian retina. J Comp Neurol 2013; 522: 1411–1443.

61. Pettigrew JD, Dreher B, Hopkins CS, et al. Peak density and distribution of ganglion cells in the retinae of microchiropteran bats: implications for visual acuity. Brain Behav Evol 1988; 32: 39–56. [PubMed: 3191381]

62. Grillo SL, Koulen P. Psychophysical testing in rodent models of glaucomatous optic neuropathy. Exp Eye Res 2015; 141: 154–163. [PubMed: 26144667]

63. Bui BV, Weisinger HS, Sinclair AJ, et al. Comparison of guinea pig electroretinograms measured with bipolar corneal and unipolar intravitreal electrodes. Doc Ophthalmol 1998; 95: 15–34. [PubMed: 10189179]

64. Racine J, Behn D, Lachapelle P. Structural and functional maturation of the retina of the albino Hartley guinea pig. Doc Ophthalmol 2008; 117: 13–26. [PubMed: 18034273]

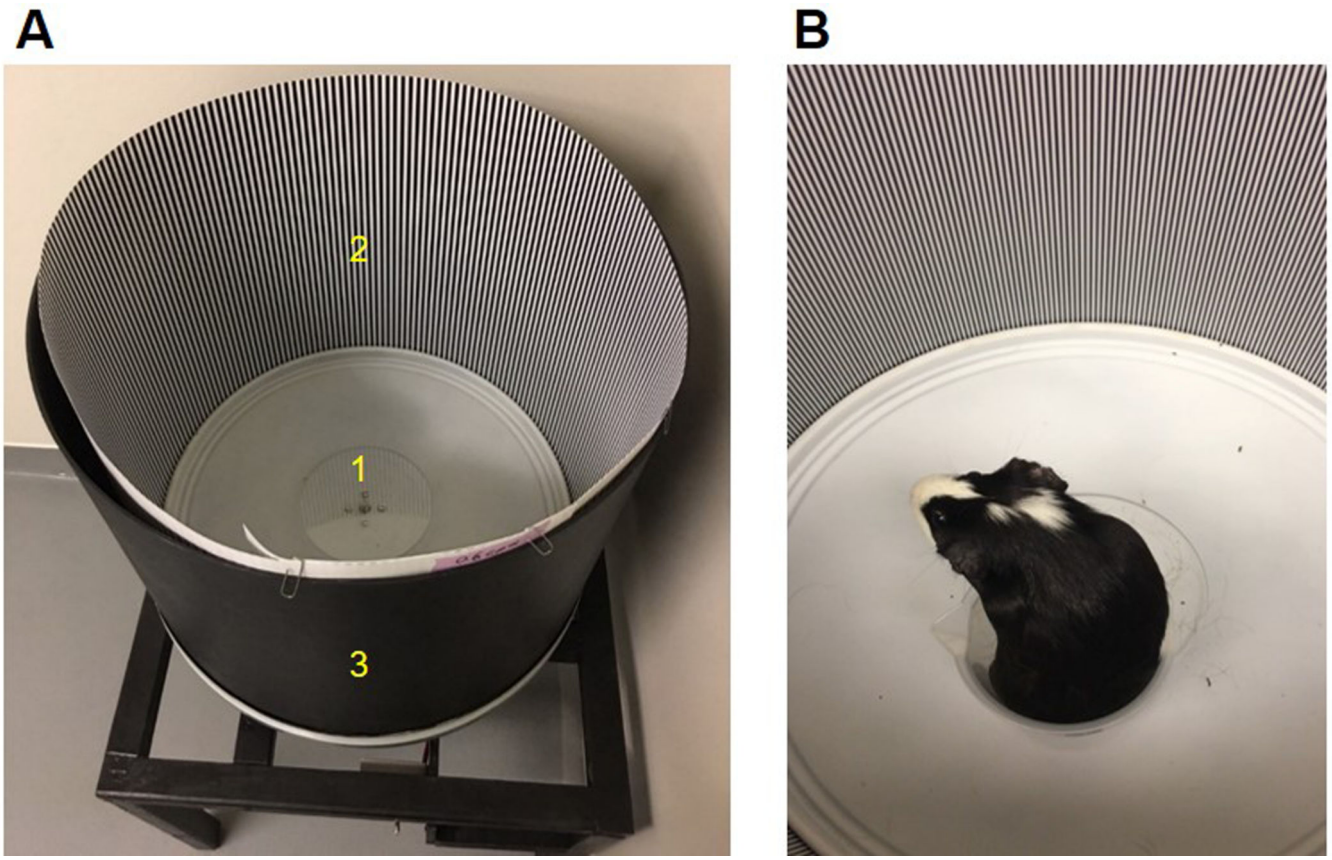

Figure 1.

A: Custom optomotor instrument. Labels indicate 1) stationary platform, 2) square wave gratings printed on photographic paper, and 3) cylindrical drum of 55 cm diameter; B: guinea pig on stationary platform in the instrument

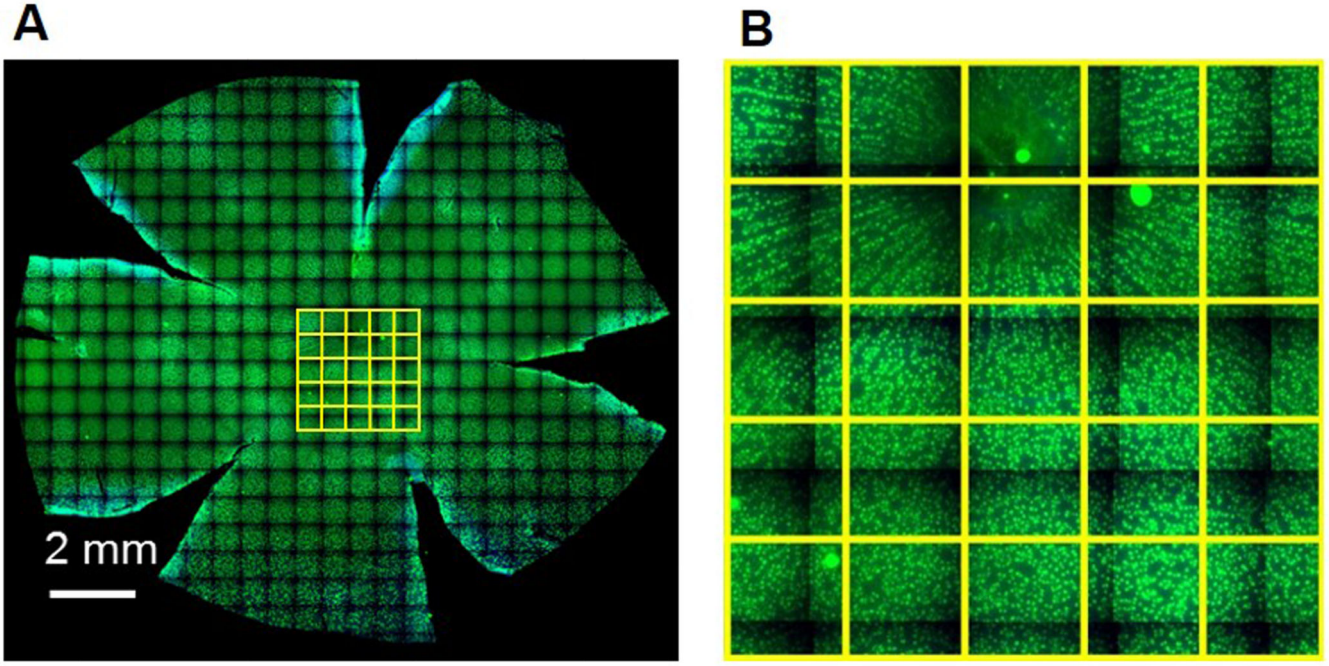

Figure 2.

A: Representative stitched image of guinea pig retinal whole mount with retinal ganglion cells labeled in green; B: magnified image of central retina from the retinal whole mount, each yellow box is 250 × 250 μm^2

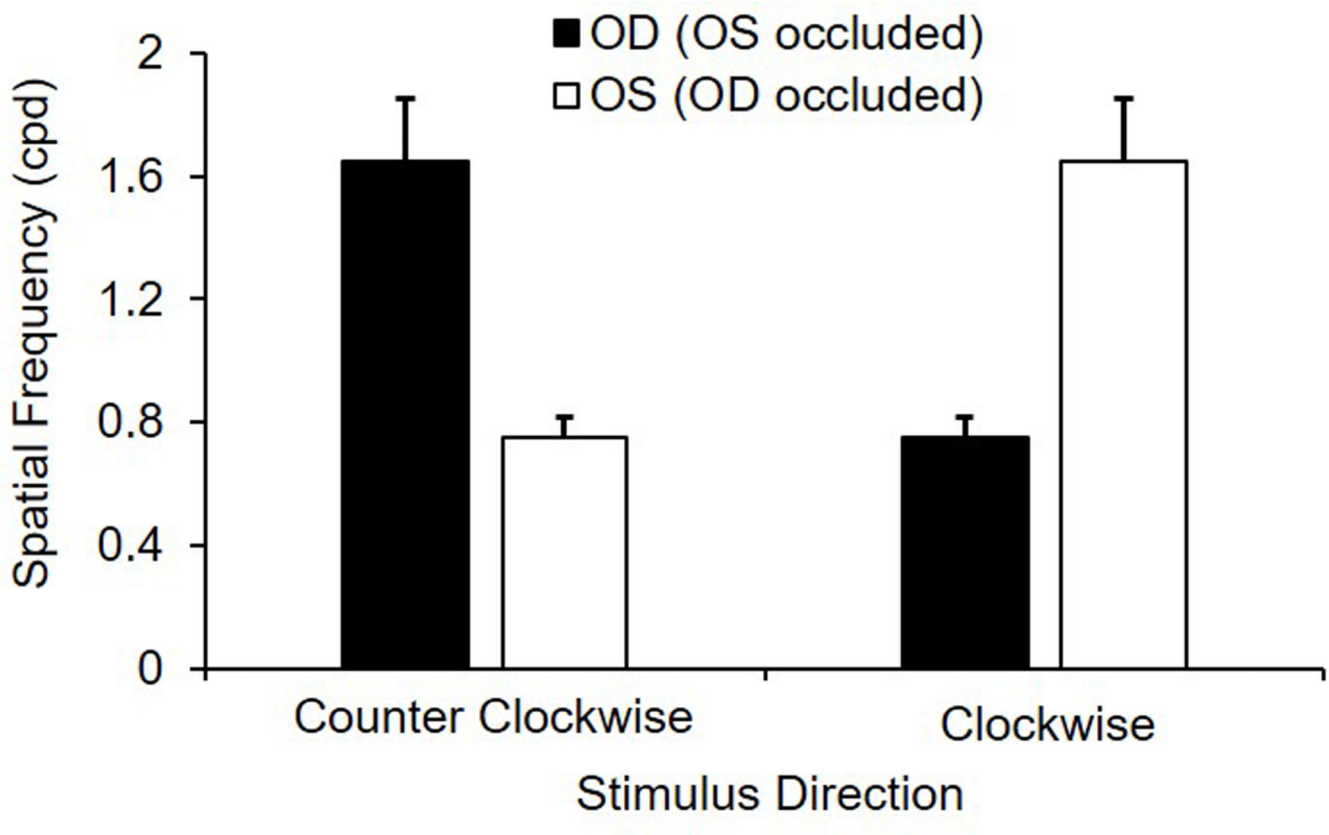

Figure 3.
Monocular spatial frequency sensitivity (cycles per degree, cpd) in adult guinea pigs (n = 6) for clockwise and counterclockwise rotating gratings

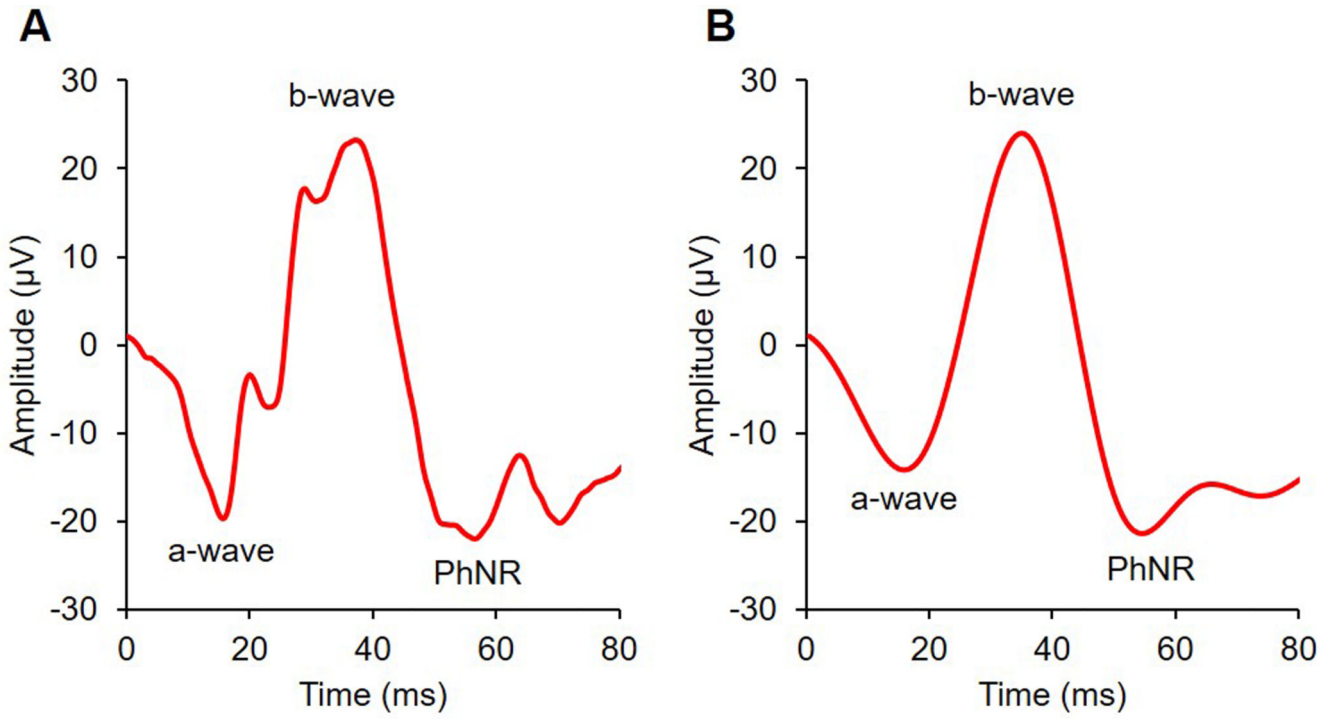

Figure 4.

A: Raw and B: filtered representative traces for a full field photopic flash ERG elicited with a 10.0 cd.s/m^2 stimulus; a-waves were derived from raw traces, and b-waves and photopic negative responses (PhNR) were derived from filtered traces

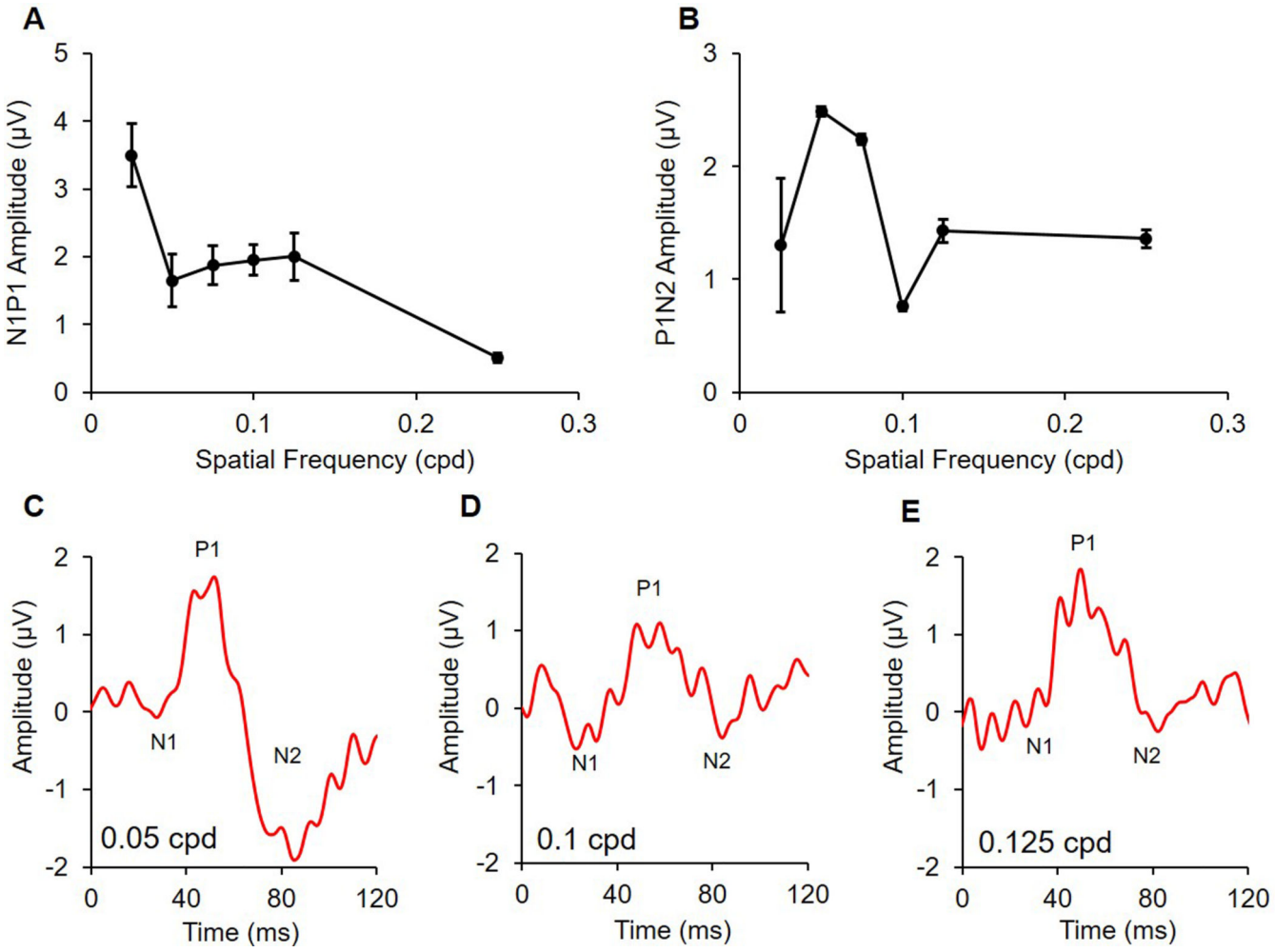

Figure 5.

A: N1P1 and B: P1N2 amplitudes in adult guinea pigs (n = 6) of the pattern ERG for alternating (1.05 Hz) square wave gratings of increasing spatial frequency; representative traces are shown for C: 0.05 cpd, D: 0.1 cpd, and E: 0.125 cpd

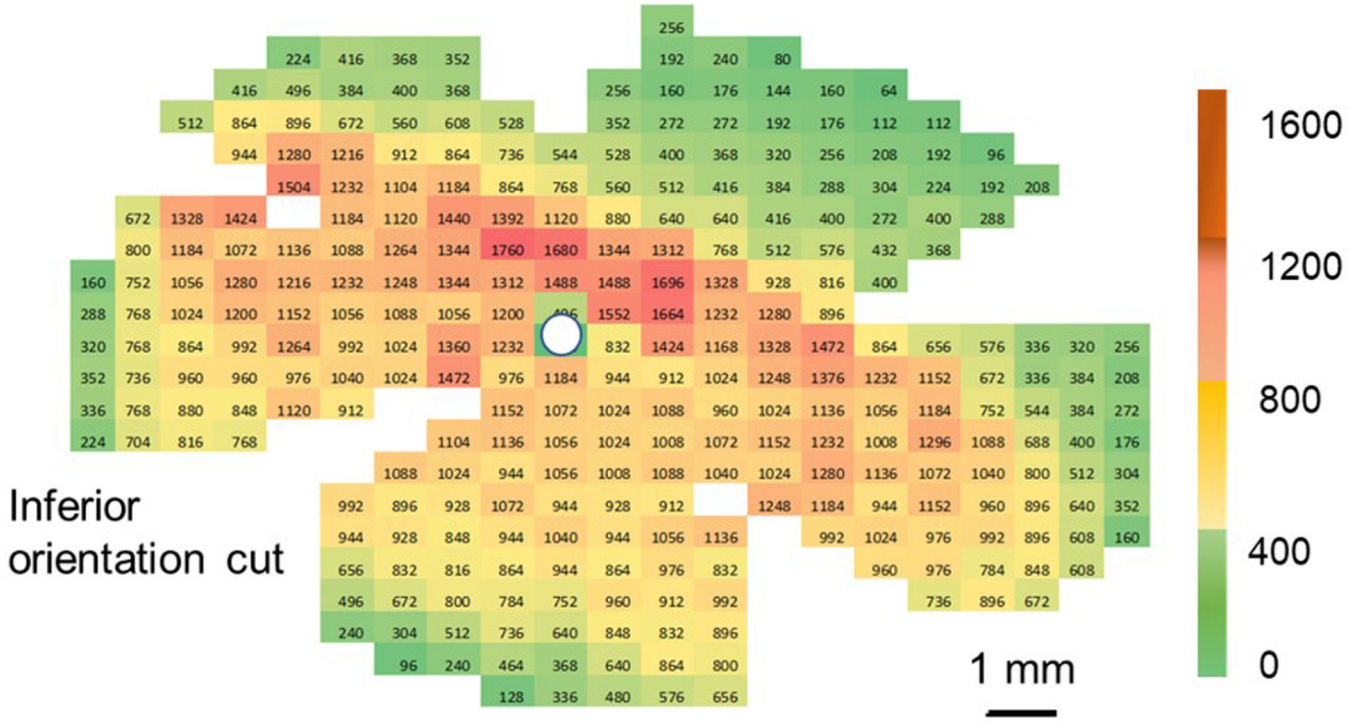

Figure 6.
Representative retinal ganglion cell density heat map for the left eye of one guinea pig (scale bar = 1 mm)

Table 1.

Amplitude (μV) and implicit times (ms) of the a-wave, b-wave, and photopic negative response (PhNR) of the full field flash ERG from adult guinea pigs (n = 6) for flash luminance energy of 10.0 cd.s/m^2

Amplitude (μV)			COV (%) (95% CI)	Implicit time (ms)		COV (%) (95% CI)
	Session 1	Session 2		Session 1	Session 2	
a-wave	18.2 ± 3.15	17.1 ± 2.8	15.4 (3.5–27.3)	13.8 ± 0.4	15.7 ± 1.4	4.5 (1.0–8.1)
b-wave	31.5 ± 6.83	29.9 ± 5.1	19.3 (4.3–34.2)	32.1 ± 0.4	35.9 ± 2.4	3.2 (0.7–5.7)
PhNR	26.0 ± 6.38	25.4 ± 5.5	22.6 (5.1–40.1)	53.5 ± 2.6	58.6 ± 8.5	7.7 (1.7–13.8)

Table 2:

Amplitude (μV) and implicit time (ms) for pattern ERG components from adult guinea pigs (n = 6) for alternating (1.05 Hz) square wave gratings of spatial frequencies ranging from 0.025 to 0.25 cycles per degree; the first negative trough (N1), positive peak (P1), second negative trough (N2), N1P1, and P1N2 are shown

Pattern ERG measures		Spatial frequency (cycles per degree)					
		0.025	**0.05**	**0.075**	**0.1**	**0.125**	**0.25**
N1	Amplitude	0.6 ± 0.5	−0.07 ± 0.2	−0.2 ± 0.3	−0.3 ± 0.4	−0.3 ± 0.3	0.2 ± 0.5
	Implicit time	27.0 ± 3.5	25.2 ± 1.8	26.8 ± 3.9	23.7 ± 4.3	25.8 ± 4.6	25.0 ± 10.5
P1	Amplitude	3.8 ± 1.1	1.9 ± 0.9	1.7 ± 0.9	1.8 ± 0.6	2.0 ± 0.9	0.5 ± 0.2
	Implicit time	54.5 ± 3.6	51.2 ± 3.6	53.5 ± 4.3	57.5 ± 5.1	55.5 ± 7.7	42.3 ± 10.5
N2	Amplitude	2.2 ± 2.6	−0.9 ± 1.1	−0.4 ± 0.9	1.2 ± 0.7	0.6 ± 0.6	−0.9 ± 0.4
	Implicit time	85.0 ± 6.6	83.3 ± 4.3	85.2 ± 3.5	86.7 ± 7.1	88.3 ± 3.7	79.8 ± 6.4
N1P1	Amplitude	3.5 ± 1.2	1.7 ± 1.0	1.9 ± 0.7	2.0 ± 0.6	2.0 ± 0.9	0.5 ± 0.2
P1N2	Amplitude	1.3 ± 1.5	2.5 ± 0.1	2.2 ± 0.2	0.8 ± 0.1	1.4 ± 0.3	1.4 ± 0.2